



# Wind Turbine Transformer Optimum Design Assuming a 3D Wound Core

Pedram Elhaminia<sup>1</sup>, Ahmad Moradnouri<sup>2</sup>, Mehdi Vakilian<sup>3</sup>

<sup>1,2,3</sup> Center of Excellence in Power System Management and Control, Electrical Engineering Department, Sharif University, Tehran, Iran.  
Email: Elhaminia@ee.sharif.edu, Moradnori@ee.sharif.edu, Vakilian@sharif.edu

## Abstract

A wind turbine transformer (WTT) is designed using a 3D wound core while the transformer's total owning cost (TOC) and its inrush current performance realized as the two objective functions in a multi-objective optimization process. Multi-objective genetic algorithm is utilized to derive Pareto optimal solutions. The effects of inrush current improvement on other operating and design parameters of the transformer such as: losses, dimensions, and weights are investigated. An approach is presented to select one design from optimal Pareto solutions based on relative improvement of the inrush current performance. Finally, this multi-objective optimum wind turbine transformer design is compared with an optimum transformer design obtained when just TOC is the objective function.

**Keywords:** Wind turbine transformer (WTT); 3D wound core; total owning cost (TOC); Inrush current; Multi-objective genetic algorithm; Pareto optimal solutions.

© 2014 IAUCTB-IJSEE Science. All rights reserved

## Nomenclature

|            |  |              |  |
|------------|--|--------------|--|
| $A$        | No-Load Loss Price [\$/W]                                | $D_{oos}$    | External Diameter of HV Winding [mm]               |
| $A_c$      | Cross Section Area of Core Limb [mm <sup>2</sup> ]       | $D_c$        | Diameter of Core Limb [mm]                         |
| $A_{HV}$   | Mean Cross Section Area of HV Winding [mm <sup>2</sup> ] | $f$          | Frequency [Hz]                                     |
| $b_w$      | Width of Core Window [mm]                                | $h$          | Height of Windings [mm]                            |
| $b_{us}$   | Width of LV Winding [mm]                                 | $h_w$        | Height of Core Window [mm]                         |
| $b_{os}$   | Width of HV Winding [mm]                                 | $I_p$        | Inrush Current Peak [A]                            |
| $B$        | Load Loss Price [\$/W]                                   | $J_{us}$     | Current Density of LV Winding [A/mm <sup>2</sup> ] |
| $B_{max}$  | Maximum Magnetic Flux Density [T]                        | $J_{os}$     | Current Density of HV Winding [A/mm <sup>2</sup> ] |
| $B_r$      | Remnant Magnetic Flux Density [T]                        | $L_{HV,air}$ | HV Winding Air-Core Inductance [H]                 |
| $B_s$      | Saturation Magnetic Flux Density [T]                     | $M_c$        | Mass of Core [kg]                                  |
| $C_{lab}$  | Labor Cost [\$]  | $M_{us}$     | Mass of LV Winding [kg]                            |
| $C_{Loss}$ | Losses Cost [\$]   | $M_{os}$     | Mass of HV Winding [kg]                            |
| $C_M$      | Material Cost [\$]                                       | $M_{yoke}$   | Mass of Core Yokes [kg]                            |
| $C_{MF}$   | Manufacturing Cost [\$]                                  | $M_{limb}$   | Mass of Core Limbs [kg]                            |
| $d_{cu}$   | Copper Mass Density [kg/m <sup>2</sup> ]                 | $N_{HV}$     | Number of Turns in HV Winding                      |
| $d_{ss}$   | Silicon Steel Mass Density [kg/m <sup>2</sup> ]          | $N_{LV}$     | Number of Turns in LV Winding                      |
| $D_{ius}$  | Internal Diameter of LV Winding [mm]                     | $P_c(B)$     | Core Loss per kg at B [W/kg]                       |
| $D_{ios}$  | Internal Diameter of HV Winding [mm]                     | $P_L$        | Load Losses [W]                                    |
| $D_{ous}$  | External Diameter of LV Winding [mm]                     | $P_{NL}$     | No-Load Losses [W]                                 |
|            |  | $PC$         | Profit Coefficient                                 |
|            |  | $q_{os}$     | HV Winding Conductor Area [mm <sup>2</sup> ]       |
|            |  | $q_{us}$     | LV Winding Conductor Area [mm <sup>2</sup> ]       |
|            |  | $R_{HV}$     | HV Winding Resistance [ohm]                        |

|                 |   |
|-----------------|---|
| $S$             | Transformer Rated Power [kVA]             |
| $\tau_{inrush}$ | Inrush Current Decay Time Constant [sec]  |
| $U_k \%$        | Short Circuit Impedance                   |
| $U_r \%$        | Resistive Part of Short Circuit Impedance |
| $U_x \%$        | Inductive Part of Short Circuit Impedance |
| $U_N$           | Volt per Turn [V]                         |
| $V_{HV,phase}$  | Phase Voltage of HV Winding [V]           |
| $\Delta$        | Distance between HV and LV Windings [mm]  |

## 1. Introduction

Wind turbine transformer (WTT), is a generator step up transformer, connecting the wind turbine to the power collection network of the wind farm [1]. WTT is a three phase dry-type or oil immersed transformer which is placed at the bottom of the wind turbine tower (inside or outside) or at the wind turbine nacelle [1]- [2].

Currently, conventional distribution transformers are widely used as WTT [2]. The wind turbine transformer constraints are not often known by the transformer manufacturers and operators and as a result using conventional distribution transformers as WTT reduces the level of reliability [1].

### A. WTT Design Challenges

Main source of the WTT's challenges is the fluctuating nature of the wind. This causes the WTT to cycle from low load to high load frequently (several times a day) imposing thermal and mechanical stress on the WTT [2]. Besides, these fluctuations demand repetitive connecting and disconnecting of the WTT which results in repetitive overvoltage transients imposing dielectric stress and repetitive inrush current imposing mechanical and thermal stress on the WTT [1]-[2]. Another effect of the variable wind speed is the rapid rise of the WTT's load to double of its rated power causing high thermal stress [3].

Second source of challenge is being supplied through a short length cable from HV side which may cause resonant overvoltages in energization [4]. Third source of challenge is being supplied through a power converter and therefore harmonic currents and high frequency voltages from LV side. Current harmonics causes overheating and thermal stresses. High frequency voltages with high value of dv/dt contributes to development of internal resonance, initiating travelling voltage surges, and application of higher stress on its insulation, [1]-[3],[5].

There are other challenges for the WTT such as turbine vibrations, low voltage fault ride through, harsh installation environment etc. [1]-[2].

Therefore the WTT is under higher electrical, mechanical and thermal stresses than a conventional distribution transformer.

On the other hand, the WTT is expected to be much more reliable and robust than a conventional distribution transformer. First reason is that the WTT is installed near the wind turbine which is a very

expensive structure and therefore it should have a higher fire proof safety characteristic when it is oil immersed [2]. Secondly the electric energy generation of the wind turbine plant should not be interrupted by occurrence of a failure in its transformer which is static equipment with lower risk and lower price. Additionally, any repair or replacing of the WTTs in the case of failure would be expensive due to the installation locations of wind farms; off-shore or remote access areas. Therefore, the WTT design should encounter a high level of reliability since its failure would lead to high economical loss [6].

Therefore, three approaches could be incorporated which are reducing the stresses, improving electrical, mechanical and thermal strength of the WTT and protecting it against damaging phenomena [7]. First two approaches are considered in this work.

### B. WTT's Inrush Current

As mentioned before, with repetitive connection and disconnection of the WTT, there is repetitive inrush current which is mainly drawn from the collection grid. This repetitive inrush current imposes thermal and mechanical stress on the WTT. Besides, it has adverse effects on the collection grid operation and on the other connected transformers. The inrush current cause voltage dip in collection grid [8] and sympathetic inrush current in other WTTs connected in parallel [9]-[10]. It would also be a problem for the auxiliary generator in energization of the islanded farm [11]. Therefore improving inrush current performance would be so beneficial both for the WTT and collection grid.

The inrush current could be reduced by some techniques in the operation phase such as controlled switching, de-energization of the transformers and pre-insertion resistors. These techniques are expensive approaches and are more suitable for power transformers [12]-[13]. Some techniques are also possible in the design phase such as interleaved winding [14] and using highly grain oriented and domain refined materials for the core [12]. Although these techniques could be utilized for inrush current reduction, they are not considered in this work.

Inrush current peak could be calculated using simple equation given in (1) ignoring winding resistance [15].

$$I_p = \frac{h}{N\mu_0} * \frac{A_c}{A_w} * (2B_n + B_r - B_s) \quad (1)$$

It could be seen that inrush current could be reduced by increasing the winding effective cross section area while decreasing the height of winding. On the other hand, decreasing the value of maximum magnetic flux density in normal transformer operating conditions is another method to reduce the inrush current peak.

In this paper, a WTT is designed while the objective function is the total owning cost which is looked to be minimized under improvement of its inrush current performance. In section II, transformer

construction is described. In section III the design algorithm is presented and in section IV, the results of study are discussed.

## 2. Transformer Construction

### A. Core

3D wound core is constructed from three wound core frames which are placed together to build the related three dimensional structure shown in Fig. 1. Benefits of this core comparing planar stacked core transformers include low no-load losses, reduced magnetic stray fields causing EMC and improved harmonic behavior [16]. This core topology has a symmetric magnetic circuit shown in Fig. 2.

Considering the equivalent magnetic circuit shown in Fig. 2 it could be concluded that the magnetic flux in the yokes of the 3D wound topology is 0.57 times the magnetic flux in the core limb by using the 3 phase circuits' concepts. On the other hand the cross section area of the yokes is half of the cross section area of the limbs and therefore the magnetic flux density in the yokes would be 1.15 times the magnetic flux density in the limbs. It means that the maximum magnetic flux density in the yokes is about 15 percent higher than the winding linkage magnetic flux density in the limbs. Therefore the no-load losses of 3D wound core transformers can be calculated using (2) [17].

$$P_{NL} = M_{limb} * P_c \left( \frac{B_{max}}{1.15} \right) + M_{yoke} * P_c (B_{max}) \quad (2)$$

The mass of 3D wound core could be calculated using (3) [17] considering the dimensions shown in Fig. 3.

$$M_c = M_{limb} + M_{yoke}$$

$$M_{limb} = (3h_w) * \left( \frac{\pi D_c^2}{4} \right) * d_{ss} \quad (3)$$

$$M_{yoke} = (3b_w + 4.86D_c) * \left( \frac{\pi D_c^2}{4} \right) * d_{ss}$$

### B. Winding

Foil winding is utilized for LV side in order to increase the short circuit mechanical strength and thermal performance of the winding [18]. Layer winding using square conductor is utilized for HV side. On the other hand, equal height is considered for LV and HV windings to decrease the axial short circuit forces on the windings [19].

### C. Oil & Insulation

The thermal stresses mainly affect the oil and the solid insulation of the WTT. Synthetic ester and



Fig. 1. 3D wound core

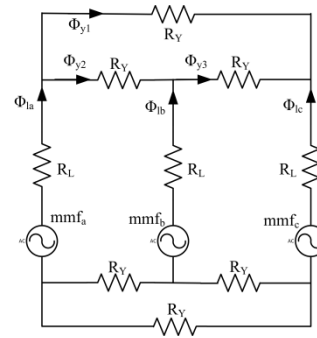


Fig. 2. Magnetic circuit of 3D wound core

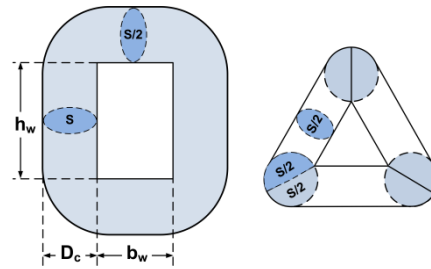


Fig. 3. Dimensions of 3D wound core

aramid insulation has high flash points and high thermal stability so they are utilized in the manufacturing phase of the WTT [20]-[21]. This insulation system increases the thermal strength, thermal stability and overload capability of the WTT.

Besides synthetic ester has high fire point, anti-oxidation properties, high moisture absorption capacity, high moisture tolerance, good biodegradability, long life, higher thermal conductivity and higher value of relative permittivity (closer to paper insulation) and higher dielectric strength [19]-[22]. Therefore using synthetic ester increases the fire safety, environmental safety, transformer life and reliability of the WTT.

## 3. Design Algorithm and Equations

Total owning cost (TOC) is one of the most widely used objective functions for the transformer optimum design. It includes both the manufacturing cost and the losses cost of the transformer. Therefore

designing a transformer with lower losses and higher material cost would become possible if it results in lower value of TOC [23].

As discussed in the introduction, inrush current performance is under attention in this work. Inrush current waveform has two basic characteristic parameters which are its maximum value and its time constant which should be considered simultaneously. To consider both parameters, square of inrush current peak multiplied by inrush current time constant which is a representation of inrush current energy is considered as another objective.

To address the two objectives; i.e., TOC and inrush current energy factor; a multi-objective optimization method should be implemented to this design process. Genetic algorithm is widely reported as a recognized method for optimum transformer design [16]. Therefore in this work a multi-objective genetic algorithm using Pareto front is utilized for optimum design of WTT. Multi-objective GA settings used for the optimum design are depicted in Table 1. Design variables are considered to be maximum magnetic flux density, LV winding current density, HV winding current density, LV winding's foil conductor thickness and its voltage per turn. The permissible range for transformer independent design variables are given in Table 2. While, the transformer design constraints are the maximum load losses, the maximum no-load losses and the short circuit impedance.

Table 1.

Multi-objective GA settings

|                    |               |
|--------------------|---------------|
| Population Type    | Double Vector |
| Population Size    | 200           |
| Creation Function  | Uniform       |
| Pareto Fraction    | 0.3           |
| Generations        | 600           |
| Crossover Function | Intermediate  |
| Selection Function | Remainder     |

Table 2.

Design variables bounds

| Parameter | Min                 | Max                 |
|-----------|---------------------|---------------------|
| $B$       | 1.2 T               | 1.8 T               |
| $J_{us}$  | 1 A/mm <sup>2</sup> | 4 A/mm <sup>2</sup> |
| $J_{os}$  | 1 A/mm <sup>2</sup> | 4 A/mm <sup>2</sup> |
| $W_{us}$  | 0.2 mm              | 2 mm                |
| $U_N$     | 5 V                 | 25 V                |

Since, in practice it is difficult to force the optimization algorithm to generate populations satisfying the constraints, a set of fitness functions are employed as defined in (4). Through application of this method, it would not be needed to compute the objective functions for designs which do not satisfy the constraints. i.e., two large values will be assigned to the two constraints not to satisfy the limit and be eliminated from the population.

$$\{F_1(X), F_2(X)\} \\ = \begin{cases} TOC, I_p^2 * \tau_{inrush} : \text{Constraints are Satisfied} \\ 1e10, 1e10 : \text{Constraints are not Satisfied} \end{cases} \quad (4)$$

For each set of variables in the population created by genetic algorithm, transformer is designed and its functional parameters are calculated. First, core limb diameter is calculated using (5).

$$D_c = \sqrt{\frac{4U_N}{4.44 * 10^{-6} * \pi * (B_{max}/1.15) * f}} \quad (5)$$

Then windings' dimensions are calculated using current densities and phase currents. After calculation of winding dimensions, other dimensions of the core including core window width and height are calculated. By deriving core dimensions, no-load losses are calculated using (2) and (3). Load losses are calculated using (6).

$$P_L = 2.4 * (M_{us} J_{us}^2 + M_{os} J_{os}^2) \quad (6)$$

The last transformer functional parameter is its short circuit impedance. The resistive part of the short circuit impedance is calculated using (7).

$$U_r (\%) = 100 * \frac{P_L}{1000 * S} \quad (7)$$

The inductive part of the short circuit impedance is calculated using (8) [15].

$$U_x (\%) = \frac{100 * (2\pi)^2 * \mu_0 * f * S}{Z * U_N^2 * (h + 0.16 * (D_{ous} - D_c))} * \\ ((D_{ius} + b_{us}) * b_{us} / 6 + (D_{ous} + 2\Delta + b_{os}) * b_{os} / 6 - \\ (D_{ous} + \Delta) * \Delta / 2 + b_{us}^2 / 12 - b_{os}^2 / 12) \quad (8)$$

Finally the short circuit impedance is calculated using (9)

$$U_k = \sqrt{U_r^2 + U_x^2} \quad (9)$$

As shown in (6), if the no-load loss, load loss and short circuit impedance are in the desired range, then TOC, inrush current peak and inrush current decay time constant are calculated. The TOC is calculated using (10) [24].

$$TOC = C_{MF} + C_{Loss} \quad (10)$$

$$C_{MF} = (1 + PC) * (C_M + C_{lab})$$

$$C_{Loss} = A * P_{NL} + B * P_L$$

To calculate the inrush current peak and its time constant, (11) to (13) could be utilized [25]-[26].

$$L_{HV,air} = 10^{-3} * \frac{\mu_0 N_{HV}^2 A_{HV}}{h} \tag{11}$$

$$I_p = \frac{\sqrt{2} * V_{HV,phase}}{\sqrt{R_{HV}^2 + (2\pi f * L_{HV,air})^2}} * (2 + \frac{B_r}{B} - \frac{B_s}{B}) \tag{12}$$

$$\tau_{inrush} = L_{HV,air} / R_{HV} \tag{13}$$

Since WTT is always energized from its HV side [3], all parameters in (11) to (13) are written with reference to the HV winding parameters. It should be mentioned that for the calculation of inrush current, remnant magnetic flux density is considered to be 0.7 of the maximum magnetic flux density.

#### 4. Design Result and Discussion

Using the abovementioned algorithm, a WTT with the specification shown in Table 3 is designed. Design assumptions are given in Table 4. The Pareto front of multi-objective design is shown in Fig. 4.

It would be useful to investigate different points on the Pareto front to see that how improvement of the inrush current has affected different parameters of the transformer. Therefore different points on Pareto optimal front are specified with numbers from 1 to 59. Higher design number is related to the design with better inrush current performance and higher TOC. Effect of the algorithm on different parameters is depicted in Fig. 5 to Fig. 12.

Considering the results, it could be concluded that:

- As it was discussed in the introduction, winding cross section is increased (Fig. 5) and winding height is decreased (Fig. 6).
- Core mass is increased since two parameters are affecting it. First increasing of core limb diameter to reduce the maximum magnetic flux density and second the increase in yoke length to consider the increase in winding diameter. (Fig. 7).
- Winding mass does not follow a general trend since its height is decreased and its diameter is increased (Fig. 8).
- Increase of core mass is simultaneous with decrease in maximum magnetic flux density.

Interaction of these two parameters first results in the decrease of no-load loss and in the last designs would result in increase of no-load loss (Fig. 9).

- The change in winding dimensions (winding height is decreased and its diameter is increased) results in higher load losses (Fig.10). It is because of higher turn length and therefore higher resistance.
- The change in winding dimensions (winding height is decreased and its diameter is increased) would increase the leakage flux considering (8). Besides the load loss is also increased and therefore the short circuit impedance is increased considering (10) (Fig. 11).
- Both costs of the transformer are increased while the losses cost has had lower changes. The reason is that no-load losses are decreased which counteracts the increase in load losses (Fig. 12).

Table 3.  
Transformer Specifications

|                             |         |
|-----------------------------|---------|
| Rated Power (kVA)           | 800     |
| LV Nominal Voltage (V)      | 690     |
| HV Nominal Voltage (V)      | 20000   |
| Frequency (Hz)              | 50      |
| Short Circuit Impedance (%) | 5.4-6.6 |
| Maximum No-Load Loss (W)    | 900     |
| Maximum Load Loss (W)       | 8500    |
| Windings Connection         | Dyn     |

Table 4.  
Design Assumptions

|                             |               |
|-----------------------------|---------------|
| Copper Price (\$/kg)        | 10            |
| Silicon Steel Price (\$/kg) | 3             |
| Load-Loss Price (\$/W)      | 2             |
| No-Load Loss Price (\$/W)   | 10            |
| Core Silicon Steel          | M2408-0.27 mm |

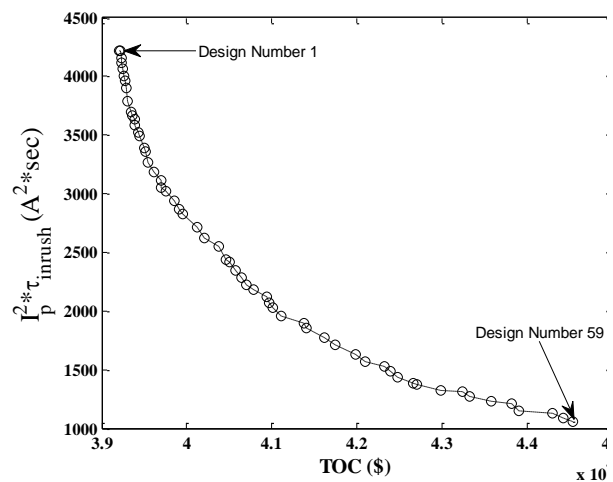


Fig. 4. Pareto front of multi-objective design

Finally one design point should be selected to satisfy the manufacturer experience concerns, the customer requirements or its field investigations concerns. One simple approach to select the optimum design point is to calculate the relative improvement obtained for inrush current while TOC of the

transformer with respect to design number 1, as a reference point, is increased. On the other hand, designer or customer may have some constraints on the improvement of inrush current energy or TOC which means that the inrush current energy improvement should be larger than a specified value

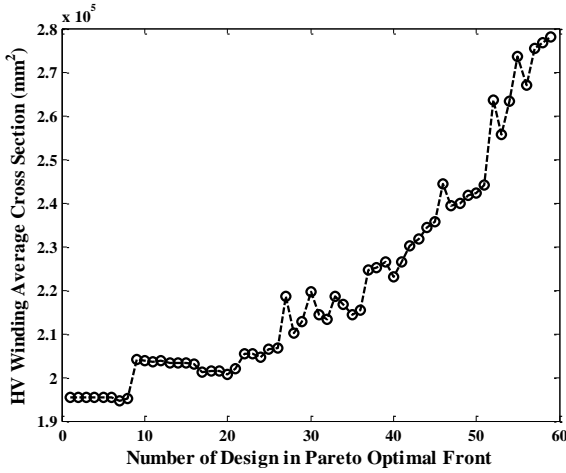


Fig. 5. Effect of inrush current improvement on HV winding cross section (higher N belongs to better inrush performance and higher TOC)

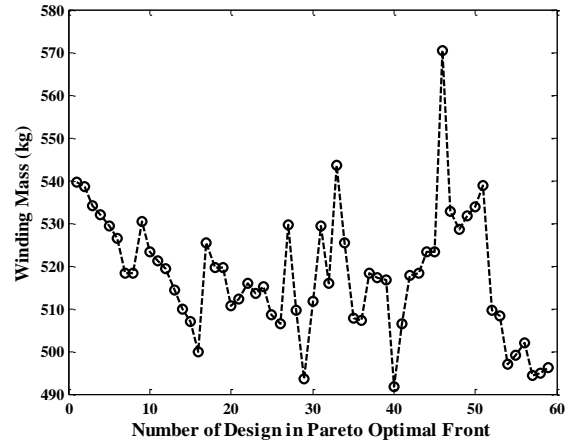


Fig. 8. Effect of inrush current improvement on winding mass (higher N belongs to better inrush performance and higher TOC)

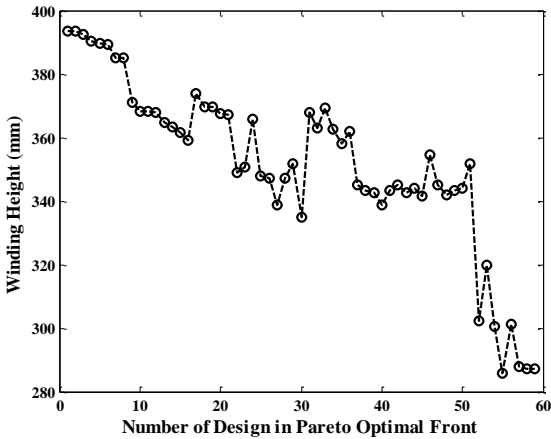


Fig. 6. Effect of inrush current improvement on HV winding height (higher N belongs to better inrush performance and higher TOC)

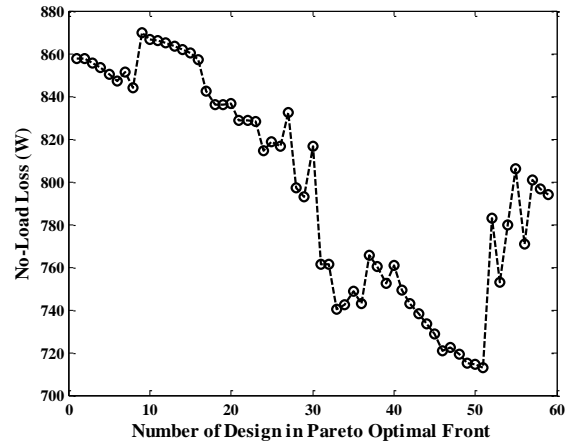


Fig. 9. Effect of inrush current improvement on no-load loss (higher N belongs to better inrush performance and higher TOC)

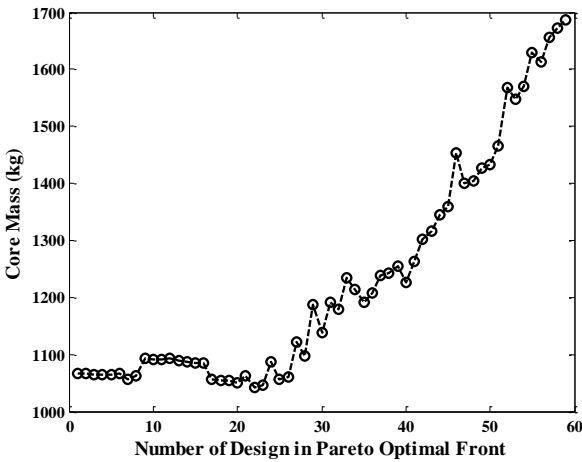


Fig. 7. Effect of inrush current improvement on core mass (higher N belongs to better inrush performance and higher TOC)

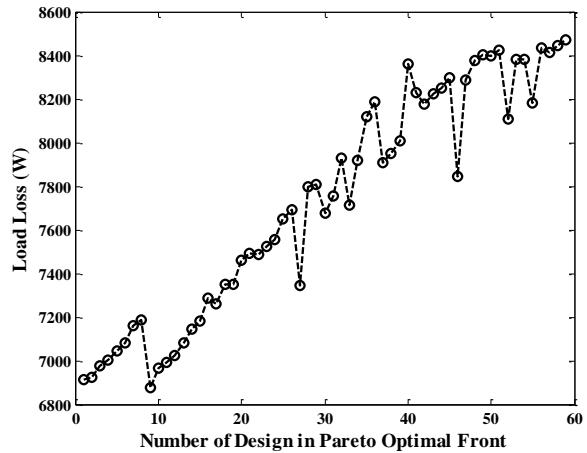


Fig. 10. Effect of inrush current improvement on load loss (higher N belongs to better inrush performance and higher TOC)

or TOC change should not surpass a pre-specified value. Relative improvements considering different objectives constraints are shown in Fig. 13.

It could be seen that by assigning different ranges to the constraints, the optimum design point could change. Reviewing all designs (shown in Fig. 13(a)), the design number 4 appears to be the best. By considering 50 percent improvement of inrush current while the TOC does not increase more than 10 percent, the best design would be design number 37. The detail information of these two designs is given in Table 5 as case II and III respectively. The optimum design with just TOC as the objective function is also given in Table 5 as case I.

Comparing these three designs together, reveals that the design number 4 and the design done with just TOC as objective function are very similar. On the other hand design number 37 has a great improvement in inrush current peak and time constant. Functional parameters of this design has suitable margin from their allowable limits.

## 5. Summary and Conclusion

A wind turbine transformer was designed using a 3D wound core, while employing copper foil for LV winding and square cross section copper for HV winding. Multi-objective optimization using genetic algorithm was implemented on inrush current performance and TOC as objective functions. It was shown that improvement of inrush current is obtained through increasing the diameter and decreasing the height of the transformer. Doing so makes no-load losses to decrease and load losses to increase. Selection of the optimum design based on relative improvement of the inrush current performance is strongly dependent on the constraints assigned by the designer or the costumer. Finally the selected design is presented and compared with the optimum design obtained only through TOC optimization and showed that a great improvement obtained in reduction of inrush current peak which improves its reliability. A next important research step in this design work is improvement of the insulation design of WTT, realizing the higher stresses on its insulation with respect to a distribution transformer of similar rating, as discussed in the introduction section.

Table 5.  
Comparison of three optimum transformer designs parameters

| Parameter | Unit              | Case I | Case II | Case III |
|-----------|-------------------|--------|---------|----------|
| $J_{us}$  | A/mm <sup>2</sup> | 2.29   | 2.45    | 2.15     |
| $J_{os}$  | A/mm <sup>2</sup> | 1.91   | 2.08    | 2.61     |
| $U_N$     | V                 | 11.5   | 11.89   | 12.15    |
| $B_{max}$ | T                 | 1.61   | 1.61    | 1.42     |
| $D_c$     | mm                | 220.4  | 223.7   | 241.6    |
| $b_w$     | mm                | 400    | 398.5   | 420.5    |
| $h_w$     | mm                | 517    | 490.7   | 445.5    |
| $N_{LV}$  | -                 | 35     | 34      | 33       |
| $q_{us}$  | mm <sup>2</sup>   | 292    | 273.3   | 310.7    |
| $h$       | mm                | 417.3  | 390.4   | 345.2    |
| $W_{us}$  | mm                | 0.70   | 0.70    | 0.90     |
| $D_{ius}$ | mm                | 230.4  | 233.7   | 251.6    |

|                 |                 |       |        |       |
|-----------------|-----------------|-------|--------|-------|
| $D_{ous}$       | mm              | 300.4 | 301.7  | 330.8 |
| $N_{HV}$        | -               | 1758  | 1707   | 1657  |
| $q_{os}$        | mm <sup>2</sup> | 6.97  | 6.41   | 5.10  |
| $D_{ios}$       | mm              | 310.4 | 311.7  | 340.8 |
| $D_{oos}$       | mm              | 395   | 393.5  | 415.5 |
| $P_{NL}$        | W               | 844.5 | 853.6  | 765.5 |
| $P_L$           | W               | 6656  | 7004.7 | 7906  |
| $U_k$           | %               | 5.51  | 5.43   | 6.31  |
| TOC             | \$              | 34211 | 34381  | 35929 |
| $I_p$           | A               | 81.21 | 80.51  | 53.24 |
| $\tau_{inrush}$ | sec             | 0.19  | 0.18   | 0.17  |

## References

- [1] IEC 60076-16, "Power Transformers- Part 16: Transformers for Wind Turbine Applications," 2011.
- [2] G. Jose and R. Chaco, "A review on wind turbine transformer", International Conference on Magnetics, Machines & Drives (AICERA-2014 iCMMD), 2014.
- [3] J. H. Harlow, Electric Power Transformer Engineering, CRC press, 2012.
- [4] A. H. Soloot, H. J. Bahirat, H. K. Hidalen, B. Gustavsen and B. A. Mork, "Investigation of resonant overvoltages in offshore wind farms- modeling and protection," International Conference on Power Systems Transients (IPST), 2013.
- [5] M.Khanali, S.Jayaram, "Dielectric frequency response of transformer insulation system under high-dV/dt stresses", International Conference on the Properties and Applications of Dielectric Materials (ICPADM) , Sydney, 2015
- [6] J.Larsen, H.C.Soerensen, E.Christiansen, S.Naef, P.Volund, "Experiences from Middelgrunden 40 MW offshore wind farm", Copenhagen Offshore Wind, October, 2205.
- [7] D. Samugala, W. Piasecki, M. Ostrogorska, M. Florkowski, M. Fluczyk and O. Granhaug, "Wind turbine transformers protection method against high-frequency transients," IEEE Transaction on Power Delivery, Vol. 30, No. 2, April 2015.
- [8] T. Ma and A. Cadmore, "System studies of voltage dips resulting from energization of mv wind turbine transformers," 18<sup>th</sup> International Conference on Electricity Distribution, Turin, June 2005.
- [9] K. S. Smith, "Transformer inrush studies for wind farm grid connections," International Conference on Power Systems Transients (IPST'05), Montreal, Canada, June 19-23, 2005.
- [10] M. Sengül, B. Alboyaci, S. oztürk and H. B. Cetinkaya, "Case study of sympathetic interaction between transformers caused by inrush transients," International Conference on Power Systems Transients (IPST'05), Montreal, Canada, June 19-23, 2005.
- [11] I. Arana, A. Hernandez, G. Thumm and J. Holboell, "Energization of wind turbine transformers with an auxiliary generator in a large offshore wind farm during islanded operation," IEEE Transaction on Power Delivery, Vol. 26, No. 4, October 2011.
- [12] N.Chiesa, "Power Transformer Modeling for Inrush Current Calculation," PhD Dissertation, NTNU, 2010.
- [13] پدram شهریاری، داریوش دربار و مجتبی رسولی، "طراحی و پیاده سازی سیستم کاهش جریان هجومی با روش تخمین شار پسماند بر روی ترانسفورماتور قدرت ۱۲۵ مگاوات آمپر،" بیست و نهمین کنفرانس بین المللی برق، تهران، ۱۳۹۳.
- [14] C. K. Cheng, J. F. Chen, T. J. Liang and S. D. Chen, "Transformer design with consideration of restrained inrush current," Elsevier Journal on Electrical Power and Energy

- Systems, 2006.
- [15] R. M. Del Vecchio, *Transformer Design Principles*, CRC Press, 2010.
- [16] T. Steinmetz, J. Smajic, S. Outten, T. Hartmann and M. Carlen, "Benefits of transformers based on 3D wound core configurations," *Cigre* 2012.
- [17] X. GUO, D. Song and L. Long, "Study of material saving effect of transformer with 3-d wound core," *5<sup>th</sup> International Conference on Electricity Distribution*, 2012.
- [18] M. J. Heathcote, *J&P Transformer Book*, Elsevier, 2007.
- [19] S. V. Kulkarni and S. A. Khaparde, *Transformer Engineering Design, Technology and Diagnostics*, 2<sup>nd</sup> ed, CRC Press, 2012.
- [20] J. Declercq, "Transformers for wind turbines need for new designs or business as usual" *17<sup>th</sup> International Conference on Electricity Distribution*, Barcelona, No. 25, 12-15 May, 2003.
- [21] J. O'Brien, M. Lashbrook and R. Martin, "Synthetic ester transformer fluid a total solution to offshore transformer technology," *European Offshore Wind Conference*, Stockholm, Sweden, 2009.
- [22] V. Dang and A. Beroual, "Comparative study of statistical breakdown in mineral, synthetic and natural ester oils under ac voltage," *IEEE Transaction on Dielectrics and Electrical Insulation*, Vol.19, No. 5, October 2012.
- [23] E. Amoiralis, M. Tsili and A. Kladas, "Transformer design and optimization: a literature survey," *IEEE Transaction on Power Delivery*, Vol. 24, No 4, October 2009.
- [24] P. S. Georgilakis, *Spotlight on Modern Transformer Design*, Springer, 2009.
- [25] Y. Wang, S. G. Abdulsalam, and W. Xu, "Analytical formula to estimate the maximum inrush current," *IEEE Transaction on Power Delivery*, Vol. 23, No. 2, pp.1266 - 1268, April 2008.
- [26] R. S. Girgis and E. G. Tenyenhuis, "Characteristics of inrush current of present designs of power transformers," *IEEE Power Engineering Society General Meeting*, 2007.